ELSEVIER

Journal of Biomechanics 38 (2005) 647–655

JOURNAL OF BIOMECHANICS

www.elsevier.com/locate/jbiomech
www.JBiomech

Wave intensity in the ascending aorta: effects of arterial occlusion

A.W. Khir[a,*], K.H. Parker[b]

[a]*Brunel Institute for Bioengineering, Brunel University, Uxbridge, Middlesex UB8 3PH, UK*
[b]*Physiological Flow Studies Group, Department of Bioengineering, Imperial College, London SW7 2AZ, UK*

Accepted 26 May 2004

Abstract

We examine the effects of arterial occlusion on the pressure, velocity and the reflected waves in the ascending aorta using wave intensity analysis. In 11 anaesthetised, open-chested dogs, snares were used to produce total arterial occlusion at 4 sites: the upper descending aorta at the level of the aortic valve (thoracic); the lower thoracic aorta at the level of the diaphragm (diaphragm); the abdominal aorta between the renal arteries (abdominal) and the left iliac artery, 2 cm downstream from the aorta iliac bifurcation (iliac). Pressure and flow in the ascending aorta were measured, and data were collected before and during the occlusion. During thoracic and diaphragm occlusions a significant increase in mean aortic pressure (46% and 23%) and in wave speed (25% and 10%) was observed, while mean flow rate decreased significantly (23% and 17%). Also, the reflected compression wave arrived significantly earlier (45% and 15%) and its peak intensity was significantly greater (257% and 125%), all compared with control. Aortic occlusion distal to the renal arteries, however, caused an indiscernible change in the pressure and velocity waveforms, and in the intensities and timing of the waves in the forward and backward directions. The measured pressure and velocity waveforms are the result of the interaction between the heart and the arterial system. The separated pressure, velocity and wave intensity are required to provide information about arterial hemodynamic such as the timing and magnitude of the forward and backward waves. The net wave intensity is simpler to calculate but provides information only about the predominant direction of the waves and can be misleading when forward and backward waves of comparable magnitudes are present simultaneously.

Keywords: Wave intensity; Wave speed; Reflected waves; Ascending aorta; Occlusion

1. Introduction

The existence of reflected waves in the arterial system has long been acknowledged (Wetterer, 1956) and many possible sources of reflections along the arterial trees have been suggested (Papageorgiou and Jones, 1988). Aortic occlusion produces a strong reflection site which can change the pattern of waves in the aorta and this study investigates the effect of arterial occlusion at different sites on the pressure, velocity and reflected waves in the ascending aorta, using wave intensity analysis.

Impedance techniques have dominated the analysis of arterial waves for the past few decades (Milnor, 1989; Nichols and O'Rourke, 1998). These techniques assume that the arterial system is periodic and linear, consider the propagation of waves as additive sinusoidal wave trains, and the results are usually presented in the frequency domain. An alternative method, wave intensity analysis, is based on the solution of the one-dimensional mass and momentum equations by the method of characteristics. Wave intensity analysis does not assume any periodicity or linearity in the arterial system, considers the propagation of waves as successive infinitesimal, incremental wave fronts and the results are presented in the time domain.

Westerhof et al. (1972) introduced a linear method based on impedance analysis for separating the

*Corresponding author. Tel.: +44-1895-274000X2951; fax: +44-1895-274608.
E-mail address: ashraf.khir@brunel.ac.uk (A.W. Khir).

0021-9290/$ - see front matter © 2004 Elsevier Ltd. All rights reserved.
doi:10.1016/j.jbiomech.2004.05.039

measured pressure and velocity into their forward and backward waveforms. Parker et al. (1988) also introduced a linear method based on the method of characteristics for the separation of pressure and velocity waves. Although both methods produce similar results for the separated waveforms, wave intensity analysis provides more information about the amount of energy carried by the waves running in the forward and backward direction. Also, because wave intensity analysis is a time-domain technique, times are readily evident in the solution. Pythoud et al. (1996) developed a non-linear technique for the separation of waves, also based on the method of characteristics, and found the difference between the theoretical results of the linear and the non-linear methods was on the order of 5–10%. Since the size of the difference between the two results was comparable to the magnitude of the experimental errors, the authors concluded that the linear separation suffices for clinical purposes.

Our experiments are modeled after a classical experiment carried out by Van Den Bos et al. (1976) in which they investigated the role of the reflected waves caused by total occlusion of the aorta on the pattern of flow and pressure in the ascending aorta, using impedance analysis. Ramsey and Sugawara (1997) have also studied the effect of aortic clamping on wave intensity, although they did not separate the waves. Thus, investigating the effect of arterial occlusion on the behavior of pressure, velocity and reflected waves in the ascending aorta, using the separation techniques of wave intensity analysis is the primary aim of this study.

2. Methods

Experiments were performed in 11 mongrel dogs (average weight 22 ± 3 kg, 7 males), anaesthetised with sodium pentobarbital, 30 mg/kg-body weight intravenously. A maintenance dose of 75 mg/h was given intravenously for the duration of the experiment. The dog was endotracheally intubated and mechanically ventilated using a constant-volume ventilator (Model 607, Harvard Apparatus Company, Millis, MA, USA). After a median sternotomy, an ultrasonic flow probe (Model T201, Transonic Systems Inc., Ithaca, NY, USA) was mounted around the ascending aorta approximately 1 cm distal to the aortic valve. ECG leads were connected to both forelegs and the left back leg. A high-fidelity pressure catheter (Millar Instruments Inc., Houston, Texas, USA) was used to measure the pressure in the aortic root as near as possible to the site of the flow probe without creating interference (a few millimetres away from the flow probe, proximal to the aortic valve). The catheter was advanced from either the right or the left brachial artery.

Snares were placed at four different sites during the preparation of each dog: the upper descending thoracic aorta at the level of the aortic valve (thoracic); the lower thoracic aorta at the level of the diaphragm (diaphragm); the abdominal aorta between the renal arteries (abdominal) and the left iliac artery, 2 cm downstream from the aorta iliac bifurcation (iliac). For each occlusion, data were collected for 30 s before the occlusion (control) and during the occlusion; 3 min after the snare was applied (Barcroft and Samaan, 1935; Van Den Bos et al., 1976). At each site, total occlusion was confirmed by observing no flow distal to the occlusion site. A time interval of 10–15 min was allowed between occlusions for returning to control conditions. In order to eliminate time effects, the sequence of occlusions was varied from dog to dog using a 4×4 Latin-square. The distances between the occlusion sites and the measurement site in the ascending aorta were measured post mortem by marking the catheter at each occlusion site as it was withdrawn from the aorta.

The circumference of the post-mortem ascending aorta was measured to convert the measured flow rate into velocity. We note that the circumference of the ascending aorta of each dog was measured at zero transmural pressure and hence the calculated diameter may be less than the actual diameter in vivo. However, In order to compensate for that difference, we did not take into account the wall thickness and assumed that the measured external radius is the correct value to be used in calculating the velocities.

The pressure catheters were calibrated prior to each experiment against a mercury manometer. Because of the possible time lag attributable to the filter in the ultrasonic flow meter, the foot of the pressure and velocity waveforms were aligned at the onset of ejection, and the lag was accounted for prior to carrying out the analysis. All data were recorded at a sampling rate of 200 Hz and stored digitally. Data were converted into ASCII format using CVSOFT (Odessa Computer Systems Ltd., Calgary, Canada) and were analysed using Matlab software (The MathWorks Inc., Natick, Mass, USA). Paired t-tests were used in all comparisons presented in this paper and $p<0.05$ was considered statistically significant.

3. Theoretical analysis

The word "wave" can have different meanings in different contexts, and so we would like to define it precisely in the context of our research. Because of the prevalence of Fourier transform methods during the last half a century, arterial waves have been thought of predominantly as sinusoidal wave trains. This is not what we mean by "wave". Instead, we consider that the arterial waveform is composed of the summation of

sequential infinitesimal wavefronts, where a wavefront is the temporal change in pressure or velocity over one sampling interval (dP and dU). These wavefronts are the elemental waves of our analysis.

The wave intensity calculated from the measured pressure and velocity waveforms represents the energy flux carried by these wavefronts as they pass by the site of measurement. As will be seen, the pattern of wave intensity in the ascending aorta during the cardiac cycle is made up of three well distinguished peaks; indicating periods during the cycle when there are significant wavefronts of similar nature. It is the macroscopic summation of these wavefronts that we will refer to as a "wave" in this paper.

Generally waves can be categorised as "forward" or "backward" depending upon their direction of travel in relation to the direction of mean blood flow. Waves can be further categorised according to their nature; a wave that increases the pressure, $dP>0$, is called a "compression" wave, while one that decreases pressure, $dP<0$, is called an "expansion" wave. The effect of the pressure on the velocity depends on the direction of the wave. A forward compression wave will cause acceleration, $dU>0$, and a backward compression wave will cause deceleration, $dU<0$. Conversely, a forward expansion wave will cause deceleration, $dU<0$, and backward expansion wave will cause acceleration, $dU>0$.

The theoretical basis of wave intensity analysis is the solution of the classical 1-D conservation of mass and momentum equations and the derivation of the following equations is found in earlier papers (Parker and Jones, 1990). The net wave intensity, dI, is

$$dI = dP\,dU, \tag{1}$$

where dP and dU are the pressure and velocity differences over one sampling period respectively. The separation of waves requires knowledge of the wave speed, which we determined using the PU-loop method (Khir et al., 2001). Briefly the water hammer equation for the forward (+) and backward (−) waves is

$$dP_{\pm} = \pm\rho c\,dU_{\pm}, \tag{2}$$

where ρ is the density of the blood and c is the wave speed. Eq. (2) can be used for determining the wave speed only if the waves passing by the measurement site are all in one direction. During the earliest part of systole, it is most likely that forward waves are the only waves in the ascending aorta, since it is too early for the arrival of reflected waves. Therefore, plotting the measured pressure against the measured velocity over the cycle we obtain a PU-loop, whose slope during the very early part of systole equals ρc. On arrival of the reflected waves, the linear relationship between pressure and velocity will no longer hold and there will be a deflection point, after which the loop becomes non-linear. This point of deflection at the end of the initial linear part of the loop is determined by eye as the sampling point at which the initial slope changes direction. We note that Dujardin and Stone (1981) used the flow-pressure loop to determine the characteristic impedance.

The pressure and velocity differences across the measured wavefronts are assumed to be the addition of the differences across the forward and backward pressure and velocity wavefronts; $dP = dP_+ + dP_-$ and $dU = dU_+ + dU_-$. This assumption enables us to write the pressure and velocity differences across the forward and backward wavefronts

$$dP_{\pm} = \frac{1}{2}(dP \pm \rho c\,dU), \tag{3}$$

$$dU_{\pm} = \frac{1}{2}\left(dU \pm \frac{dP}{\rho c}\right). \tag{4}$$

The intensities of the forward and backward waves can then be written as

$$dI_{\pm} = \pm\frac{1}{4\rho c}(dP \pm \rho c\,dU)^2. \tag{5}$$

Note that the wave intensity is always positive for forward waves and negative for backward waves. The duration of the reflected wave is calculated as the period between the start (onset) and end of the separated backward intensity (dI_-). The onset and end times of the separated backward intensity were determined as the times of the first and last sampling points when (dI_-) is substantially bigger than the noise level determined from the initial part of the curve.

The separated forward and backward pressure waveforms are obtained by integrating the calculated dP_+ and dP_- from (3)

$$P_+(t) = P_0 + \sum_{\tau=0}^{t} dP_+(\tau),$$

$$P_-(t) = \sum_{\tau=0}^{t} dP_-(\tau), \tag{6}$$

where P_0 is an integration constant, chosen to be the pressure at $t=0$, which is the time of the peak of the R wave of the ECG and T is the total time of the cardiac cycle between two consecutive R waves. Similarly, the separation of the measured velocity into its forward and backward waveforms, U_+ and U_- is obtained by integrating the calculated values of dU_+ and dU_- from (4)

$$U_{\pm}(t) = \sum_{\tau=0}^{t} dU_{\pm}(\tau), \tag{7}$$

where the velocity at $t=0$ is assumed to be zero.

4. Results

4.1. The effect of arterial occlusion on pressure and flow

Fig. 1a,b shows a typical pressure and velocity waveform recorded in the ascending aorta before and during thoracic occlusion. Values of pressure and velocity during control conditions and during the different occlusions are given in Table 1.

Pressure. Systolic pressure increased by 46% during thoracic occlusion, 23% during diaphragm occlusion and 4% during abdominal occlusion. Diastolic pressure followed a similar pattern to systolic pressure and increased by 49% during thoracic occlusion and 32% during diaphragm occlusion. Mean aortic pressure calculated from the integral over the cardiac cycle increased by 45% during upper thoracic and 10% during diaphragm occlusion. The more distal occlusions resulted in no significant changes in systolic, diastolic or mean pressure.

Flow. Maximum aortic flow-rate decreased by 23% during thoracic occlusion, by 17% during diaphragm occlusion, by 5% during abdominal occlusion and by 5% during iliac occlusions. Mean aortic flow decreased by 27% during thoracic and by 25% during diaphragm occlusions. The more distal occlusions resulted in no significant changes in mean aortic flow.

4.2. The effect of arterial occlusion on wave speed and separation

The wave speed in the ascending aorta determined by the PU-loop method increased by 25% (7.9 ± 1.5 vs. $6.3 \pm 1.5\,\mathrm{m/s}$) during thoracic occlusion and by 10% (5.6 ± 0.9 vs. $5.1 \pm 1.2\,\mathrm{m/s}$) during diaphragm occlusion, compared with control values. The values of the wave speed determined for each condition were used to separate the measured pressure and velocity into their forward and backward waves using (6), (7). Fig. 2 shows the wave speed measured by the PU-loop measured in the ascending aorta during control and during thoracic occlusions in a typical dog. Fig. 3 shows the results of the separation of forward and backward waves during control and diaphragm occlusion. The onset of the backward pressure and velocity waveforms, P_- and U_-, corresponds to the arrival of the reflected wave detected by the backward wave intensity, $\mathrm{d}I_-$, and is indicated by the vertical dotted line. The sizes of the backward pressure (P_-), velocity (U_-) and wave intensity ($\mathrm{d}I_-$) during the occlusion are higher than those under control conditions. Note that the measured pressure and velocity waveforms, P and U, remained similar in shape to the separated forward pressure and velocity, P_+ and U_+ until the arrival of the reflected waves.

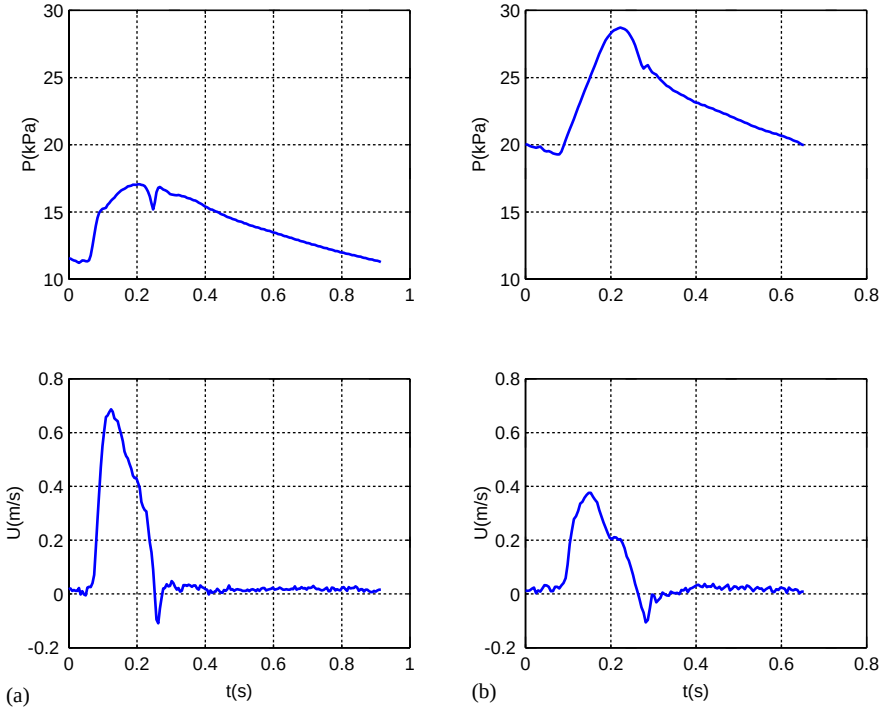

Fig. 1. Pressure and velocity waveforms for one beat measured in the ascending aorta of an open chest dog during (a) Control and (b) Thoracic occlusion. Note the increase of systolic pressure and decrease of flow during occlusion.

Table 1
The effect of arterial occlusion on the pressure and flow-rate in the ascending aorta

	Thoracic		Diaphragm		Abdominal		Iliac	
	Control	During	Control	During	Control	During	Control	During
P_s (kPa)	15.5±2.6	22±4.9[a]	P15.9±1.7	19.5±2.2[a]	14.7±1.2	15.2±1.8[a]	14.6±2.1	14.6±2
P_d (kPa)	9.8±1.8	14.6±3.5[a]	10.5±1.3	13.8±2.6[a]	9.3±1.5	9.9±1.6	9.1 ±2.5	9.8±1.8
P_m (kPa)	12.8±1.8	18.7±3.3[a]	15±2.5	16.6±2.2[a]	12.7±1.7	13.6±2.5	12.6±2.1	12.7±2.1
Q_{max} (l/min)	7.2±2.8	5.5±2.8[a]	7.4±2.4	6.1±2.4[a]	6.8±2.6	6.5±2.7[a]	7.4±2.3	7.0±2.4[a]
Q_m (l/min)	1.3±0.6	0.9±0.5[a]	1.2±0.5	0.9±0.4[a]	1.2±0.63	1.2±0.57	1.2±0.54	1.2±0.53

P_s = Systolic pressure. P_d = Diastolic pressure. P_m = Mean pressure. Q_{max} = Maximum aortic flow-rate. Q_m = Mean aortic flow-rate (cardiac output).
[a]Significantly different from control conditions.

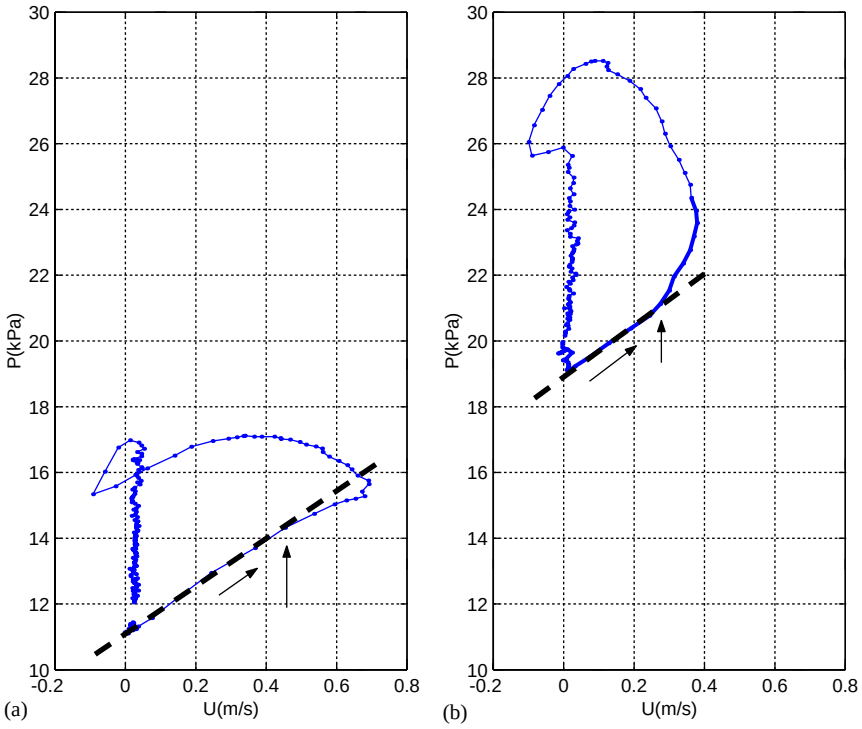

Fig. 2. The *PU*-loop method for measuring wave speed during (a) Control conditions and (b) Thoracic occlusion. The slope of linear part of the loop (dotted line) equals ρc and the diagonal arrows indicate the direction of the loop. The vertical arrows indicate the deflection point at which the loop deviates from its initial linear behaviour.

4.3. The effect of arterial occlusion on wave intensity

The reflected wave is interpreted as the resultant of all the reflected wavefronts arriving back at the ascending aorta from reflection sites distributed along the circulation. Total occlusion of the aorta created a strong reflection site and a substantially greater reflected wave for the proximal occlusions was observed more than that observed under control conditions. During thoracic and diaphragm occlusions, the reflected waves arrived back to the aortic root earlier, their duration increased and their maximum intensity was greater. Fig. 4 shows a comparison of the size, time and duration of the wave intensities before and during thoracic occlusion in a typical dog.

The results of the wave intensity analysis during control conditions and during the occlusions are given in Table 2. The peak of the reflected wave was largest with thoracic occlusion and decreased as the occlusion site moved distally, so that during iliac occlusion it became indiscernibly different from that of control. The peak of the compression and expansion forward waves decreased significantly with thoracic and diaphragm occlusions, and to a lesser degree during abdominal

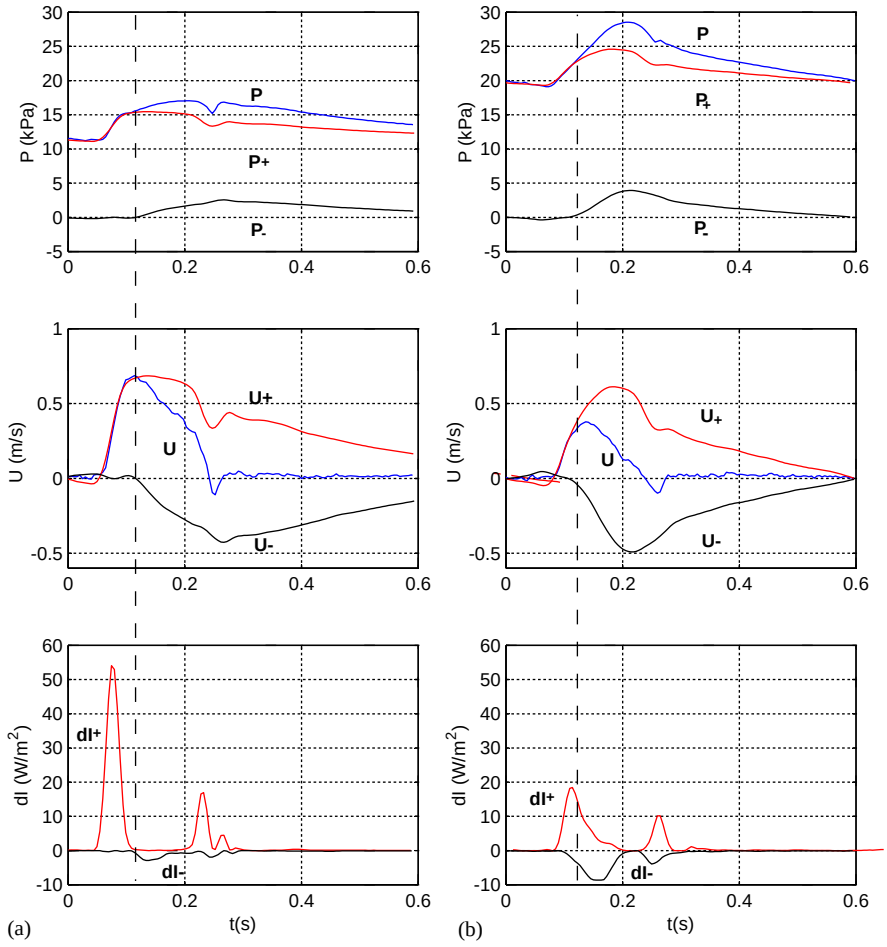

Fig. 3. The separation of the measured pressure and velocity into their forward and backward waveforms during (a) Control and (b) Thoracic occlusion, are shown in the top two panels. In the bottom panel, wave intensity is also separated into its forward and backward intensities. The arrival time of the reflected waves detected by the onset of dI_- corresponds to the onset of the backward pressure and velocity waves as indicated by the vertical dotted line.

and iliac occlusions, compared with control conditions. Fig. 5 shows the size of the forward and backward wave intensities during control condition and with an occlusion at different sites.

5. Discussion and conclusions

Wave intensity analysis has a number of distinctive advantages: (a) the method is a time domain analysis, which makes it easier to relate times directly to physiological events.; (b) no assumption is made about periodicity or linearity; (c) the analysis can accommodate viscoelastic, convective and friction effects. The units of wave intensity, (W/m^2) have a physical meaning; the energy flux carried by the wave per unit area of the artery. Ramsey and Sugawara (1997) suggested a variant of the analysis using the traditional differential with respect to time, calculated by dividing dP and dU by the sampling time so that Eq. (1) is written $dI = \frac{dP}{dt}\frac{dU}{dt}$. The units of the modified equation are $(W/m^2\,s^2)$, which lack an obvious physical meaning. On the other hand, their definition has the advantage that the computed wave intensity is independent of the sampling rate.

The measured pressure and velocity waveforms are the result of the interaction between the heart and the arterial system. The pressure and velocity waveforms are two different facets of the same pulse wave generated by ventricular contraction. Pressure and velocity waveforms measured in the ascending aorta are different from each other in shape because of the effects of the reflected waves. In a hypothetical frictionless and reflectionless system, we would expect to measure a similar shape of pressure and velocity waveforms all along the aorta. Note that the separated forward pressure and velocity waveforms, P_+ and U_+ seen in Fig. 3 are identical in shape.

The arrival time of the reflected waves to the ascending aorta is of physiological importance. If the

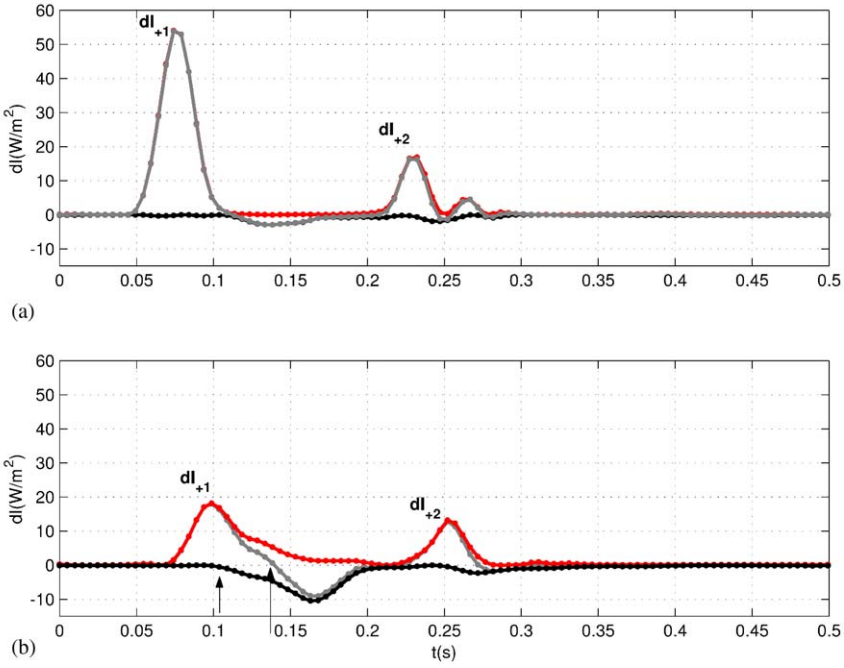

Fig. 4. The separated wave intensity calculated from pressure and velocity measured in the ascending aorta of dog during (a) Control and (b) Thoracic occlusion. dI_{+1} is the peak of the forward compression wave and dI_{+2} is the peak of the forward expansion wave. The reflected wave arrives earlier, its duration is longer and its magnitude is larger during occlusion. The arrows point to the onset of the reflected waves as determined by wave intensity: short arrow, separated backward intensity, dI_- and long arrow, net intensity dI. Note the decrease in the size of dI_{+1} and dI_{+2} during occlusion.

Table 2
The effect of occlusion on waves in the ascending aorta

	Thoracic		Diaphragm		Abdominal		Iliac	
	Control	During	Control	During	Control	During	Control	During
dI_{+1} (W/m^2)	37±33	22±20[a]	31±15	30±12[a]	39±41	38±40	37±26	34±25
dI_{+2} (W/m^2)	19±8	11±6[a]	22±11	17±10[a]	18±9	15±7[a]	21±13	19±15[a]
dI_- (W/m^2)	1.8±0.8	6.5±6.3[a]	2.5±1.1	5.7±3.3[a]	2.1±1.4	2.0±1.8	2.1±0.7	2.3±0.9
t_- (ms)	65±7	28±4[a]	67±8	57±5[a]	64±9	63±8	63±7	65±6
L_m (cm)	—	12.5±1.2	—	24.9±1.7	—	38.7±1.9	—	51±2.1
L_c (cm)	27±2	12.3±1	28.5±2	24.5±2	27.5±2	29±2	28.5±3	30±3

dI_{+1} = Peak of the forward compression wave. dI_{+2} = Peak of the forward expansion wave, dI_- = Peak of the reflected wave, t_- = Arrival time of the reflected wave, L_m = Measured distance to the occlusion site and L_c = Calculated distance to the closest occlusion site. Sampling rate is 200 Hz.
[a]Significantly different from control conditions.

reflected compression wave arrives before the aortic valve is closed, left ventricular afterload will be increased, since the left ventricle will be required to produce extra work to overcome the increase in pressure associated with the backward compression waves. The onset of the reflected wave was determined as the time of the first sampling points when dI_- is substantially bigger than the noise level determined from the initial part of the curve. Under control conditions, the reflected wave returns to the ascending aorta after the end of the initial forward compression wave and its timing can be determined from the net wave intensity, dI as seen in Fig. 4a. Under occlusion conditions wave reflections arrive during the initial compression wave, and so using the net wave intensity to determine the timing and magnitude of the reflected wave can be very misleading as seen in Fig. 4b.

Wave intensity analysis can be used to estimate the distance to the reflection sites. The temporal difference between the beginning of the forward compression wave

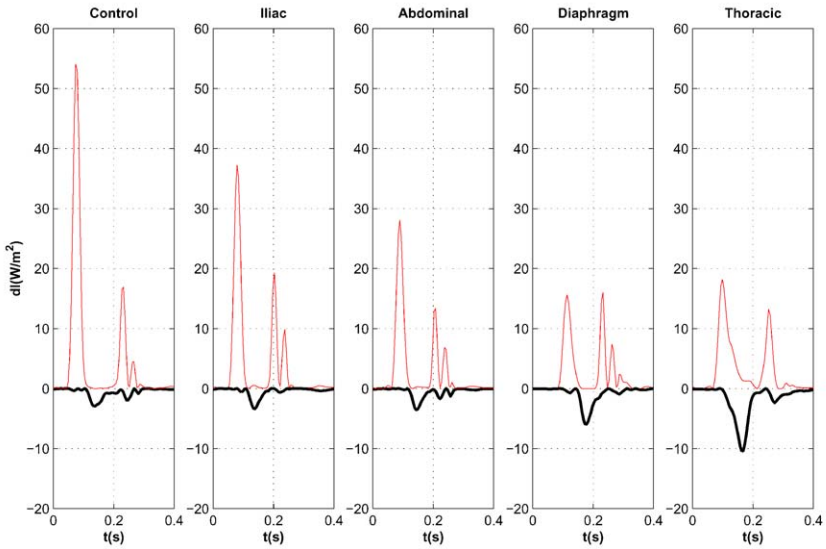

Fig. 5. The forward and backward wave intensities determined by wave intensity analysis during control conditions and during the different occlusions. Zero time is the peak of the QRS wave. While the magnitude of the reflections during iliac and abdominal occlusions are not discernibly different from those during control, the reflections during diaphragm and thoracic occlusions were much greater. Note the earlier arrival and longer duration of the reflected waves during diaphragm and thoracic occlusions compared with those at control conditions. Also note the gradual decrease in the size of the forward compression and expansion waves.

and the arrival of the backward compression wave is the time that it takes for the wave to travel downstream, be reflected and arrive back at the measurement site in the ascending aorta, ($2\Delta t$). If the wave speed is known, we can then calculate the distance to the reflected site, $L = c\Delta t$. For example, the measured (post mortem) occlusion site in the example shown in Fig. 4b is 14.5 cm and the onset of the reflected wave from the calculated backward wave intensity, dI_-, is 39 ms. The wave speed in the ascending aorta of this dog, measured by the PU-loop during thoracic occlusion is 7.2 m/s and so the calculated occlusion distance is 14 cm. It is worth noting that wave speed is a local mechanical property of the vessel and generally increases with distance along the aorta (Latham et al., 1985). Therefore, estimates of distances along the aorta based on a uniform wave speed will probably lead to under-estimation.

The ability of the separated wave intensity to detect the distance to the occlusion site in a long elastic tube where there was only one reflection site has been previously demonstrated (Khir and Parker, 2002). However, in the present experiments the arterial system will certainly have many reflection sites as well as the occlusion of the aorta. We believe that in the proximal occlusions, the main reflection site was that of the occlusion, which is consistent with the results of earlier arrival and larger size of the reflected waves compared with control. However, with the distal occlusions, neither the arrival time nor the size of the reflection was different from that of the control, which was somewhat surprising. Other researchers observed similar behaviour and have shown that waves produced artificially in the distal circulation have no discernible influence on the ascending aortic pressure waveform (Starr et al., 1953; Peterson and Shepard, 1955). A possible explanation for this observation is that waves reflected from the lower occlusions become very small in magnitude by the time they arrive back to the ascending aorta. One of the reasons for the decreased magnitude of these reflected waves could be the mismatched arterial bifurcations in the backward direction, since the arterial bifurcations are known to be well-matched only in the forward direction (Pedley, 1980). Reflected waves arising from the occlusion of the aorta below the diaphragm level will be re-reflected (in the forward direction) and the magnitude of the transmitted wave (in the backward direction) will be decreased in magnitude. If the reflected wave passes through a number of consecutive junctions, generating re-reflections at each of them, we expect the reflected wave arriving to the ascending aorta to be very small in magnitude (Wang and Parker, 2004).

We conclude that the separated pressure, velocity and wave intensity are required to provide information about arterial hemodynamic such as the timing and magnitude of the forward and backward waves. The net wave intensity is simpler to calculate but provides information only about the predominant direction of the waves and can be misleading when forward and backward waves of comparable magnitudes are present simultaneously.

Acknowledgements

We would like to thank Professor JV Tyberg for offering the experimental facilities used to obtain the data. We also acknowledge the excellent technical support received from Ms. Rozsa Sas, Ms. Cheryl Meek and Mr. Gerald Groves. Ashraf Khir was supported by the Special Cardiac Fund of Royal Brompton Hospital and received a doctoral scholarship from the Christ Foundation, to which he is very grateful.

References

Barcroft, H., Samaan, A., 1935. The explanation of the increase in systemic flow caused by occluding the descending thoracic aorta. Journal of Physiology 85, 47–61.

Dujardin, J.P., Stone, D.N., 1981. Characteristic impedance of the proximal aorta determined in the time and frequency domain: a comparison. Medical & Biological Engineering & Computing 19, 565–568.

Khir, A.W., Parker, K.H., 2002. Measurements of wave speed and reflected waves in elastic tubes and bifurcations. Journal of Biomechanics 35, 775–783.

Khir, A.W., O'Brien, A., Gibs, J.S.R., Parker, K.H., 2001. Determination of wave speed and wave separation in the arteries. Journal of Biomechanics 34, 1145–1155.

Latham, R.D., Westerhof, N., Spikema, P., Rubal, B.J., Reuderink, P., Murgo, J.P., 1985. Regional wave travel along the human aorta: a study with six simultaneous micromanometric pressures. Circulation 72, 1257–1269.

Milnor, W.R., 1989. Hemodynamics. Williams and Wilkins, Baltimore, MD.

Nichols, W.W., O'Rourke, M.F., 1998. McDonald's Blood Flow in Arteries (4th Ed.). Edward Arnold, London.

Papageorgiou, G.L., Jones, N.B., 1988. Wave reflection and hydraulic impedance in the healthy arterial system: a controversial subject. Medical & Biological Engineering & Computing 26, 237–242.

Parker, K.H., Jones, C.J., 1990. Forward and backward running waves in the arteries: analysis using the method of characteristics. Journal of Biomechanical Engineering 112, 322–326.

Parker, K.H., Jones, C.J., Dawson, J.R., Gibson, D.G., 1988. What stops the flow of blood from the heart? Heart Vessels 4, 241–245.

Pedley, T.J., 1980. The Fluid Mechanics of Large Blood Vessels. Cambridge University Press, London.

Peterson, L.H., Shepard, R.B., 1955. Symposium on applied physiology in modern surgery: some relationships of blood pressure to the cardiovascular system. Surgical Clinics of North America 35, 1613–1628.

Pythoud, F., Stergiopulos, N., Meister, J.-J., 1996. Separation of arterial pressure into their forward and backward running components. Journal of Biomechanical Engineering 118, 295–301.

Ramsey, M.W., Sugawara, M., 1997. Arterial wave intensity and ventricular interaction. Heart Vessels 12, 128–134.

Starr, I., Schnabel, Jr., T.G., Mayock, R.L., 1953. Studies made by simulating systole at necropsy II. Experiments on the relation of cardiac and peripheral factors to the genesis of the pulse wave and the ballistocardiogram. Circulation 8, 44–61.

Van Den Bos, G.C., Westerhof, N., Elzinga, G., Sipkema, P., 1976. Reflection in the systemic arterial system: effects of aortic and carotid occlusion. Cardiovascular Research 10, 565–573.

Wang, J.J., Parker, K.H., 2004. Wave propagation in a model of the human arterial system. Journal of Biomechanics 37, 457–470.

Westerhof, N., Sipkema, P., Van Den Bos, G.C., Elzinga, G., 1972. Forward and backward waves in the arterial system. Cardiovascular Research 6, 648–656.

Wetterer, E., 1956. Die Wirkung der Herztatigkeit auf die Dynamik des Arteriensystems. Verhandlungen der Duetchen Gesellschaft fur krieslaufforschungen 22, 26–60.